River Flow 2010 - Dittrich, Koll, Aberle & Geisenhainer (eds) - © 2010 Bundesanstalt für Wasserbau ISBN 978-3-939230-00-7

2-D numerical modeling of rapidly varying shallow water flows by Smoothed Particle Hydrodynamics technique

R. Vacondio & P. Mignosa
DICATeA, University of Parma, v.le G. Usberti 181/A, 43100 Parma, Italy

B.D. Rogers & P.K. Stansby
School of Mech. Aero. & Civil Engng., The University of Manchester, Manchester, M60 1QD, UK

ABSTRACT: Smoothed Particle Hydrodynamics for shallow water flow problems has received some attention since it is an attractive mesh-free, automatically adaptive method without special treatment for wet/dry interfaces. In this paper an algorithm for particle splitting is introduced in order to avoid low resolution at small depths, and a new procedure for discretizing the bed source term in presence of irregular bathymetries is applied. The numerical method is tested against the reference solution for a Cylindrical Dam break over a non-flat bottom. The CADAM and the 2D Dam breaks experimental test are also reproduced in order to show the capability of the numerical method to simulate real phenomena.

Keywords: Smoothed Particle Hydrodynamics, Shallow Water Equations, Refinement, Slope source term

1 INTRODUCTION

The 2-D Shallow-Water Equations (SWEs) are a widely used description of flows over shallow domains for a great range of rapidly (and slowly) varying free surface flows, as for example, dam break flood waves, flood waves in rivers, tides in estuaries, etc.. Recently SPH methods have been applied to the SWEs (Rodriguez-Paz & Bonet 2005 and De Leffe et al. 2008) obtaining promising results; these Lagrangian models have some distinct advantages: no mesh is needed, the wet/dry interfaces require no special treatment and the mass is automatically conserved.

In this work a 2D shallow water code based on the SPH interpolation is derived with two major improvements in order to simulate real flooding test cases: following the idea of adaptive refinement usually adopted in Eulerian models a particle splitting procedure is introduced in our SPH-SWEs code with the aim of varying the resolution over the domain. Moreover a set of bottom particles is used to describe the slope source term and this allows the method to be applied to arbitrarily irregular bathymetries.

2 NUMERICAL MODEL

The SWEs are formally identical to the Euler equations if we re-define the density ρ as the amount of fluid per unit of area in a 2-D domain; given this new definition of ρ we can connect it to the depth of water d with: $\rho = \rho_w d$, where ρ_w denotes the constant 3D (conventional) density. The density ρ_i of a particle i can vary enormously during a simulation; therefore an SPH scheme with variable smoothing length h in time and space is used in order to keep the number of neighbor particles roughly constant during the processes of water inundation and retreat.

Using these definitions and the Lagrangian derivatives the SWEs can be written as follow:

$$\begin{aligned} \frac{\mathrm{d}\rho}{\mathrm{d}t} &= -\rho\nabla\cdot\mathbf{v} \\ \frac{\mathrm{d}\mathbf{v}}{\mathrm{d}t} &= -\frac{g}{\rho_w}\nabla\rho + g\left(\nabla b + \mathbf{S}_f\right) \end{aligned} \tag{1}$$

where $\mathbf{v}$ is the horizontal velocity vector, b is the bottom elevation, g is the acceleration due to gravity and $\mathbf{S}_f$ is the bed friction source term. The particles' position and the velocities are integrated in time by means of a leap-frog scheme and a Lax-Friedrichs term is used in order to keep the solution stable even in presence of shock waves (Vacondio et al. 2009a). The closed boundaries

are described using the Modified Virtual Boundary Particle method that is able to keep an approximate zero consistency in presence of complicated boundaries (Vacondio et al. 2009b).

2.1 *Density evaluation*

The SPH approximation for the density of the *i*-th particle ρ_i (Monaghan 1992) is:

$$\rho_i = \sum_j m_j W_i(\mathbf{x}_j, h_i) \tag{2}$$

where W is the cubic kernel function, $\boldsymbol{x_j}$ and m_j are the position vector and the mass of the *j*-th particle and h_i is the smoothing length. In general, h is connected to the density (Benz 1990) with:

$$h_i = h_0 \left(\frac{\rho_0}{\rho_i} \right)^{1/d_m} \tag{3}$$

where d_m is the number of dimension (1 in 1D and 2 in 2D), ρ_0 and h_0 are the density and the smoothing length at the beginning of the simulation.

The above equation is implicit because the density is itself a function of h_i as reported in Equation (3). In this paper a simple Newton - Raphson iteration is adopted in order to solve this system of Equations (2) and (3) (see Rodriguez-Paz & Bonet 2005 for details).

2.2 *Momentum equation*

Herein we follow the derivation of Rodriguez-Paz & Bonet 2005 by considering the continuum as an Hamiltonian system of particles. The Euler – Lagrange equation for each particle is:

$$\frac{d}{dt}\frac{\partial L}{\partial \mathbf{v}_i} - \frac{\partial L}{\partial \mathbf{x}_i} = 0 \tag{4}$$

where the Lagrangian functional L is defined in term of kinetic energy K and potential energy π as: $L = K - \pi$. π is a function of particles position but not of velocity, so substituting this expression into Equation (4) leads to:

$$\frac{d}{dt}\frac{\partial K}{\partial \mathbf{v}_i} - \frac{\partial K}{\partial \mathbf{x}_i} = \frac{\partial \pi}{\partial \mathbf{x}_i} \tag{5}$$

In the SPH formalism of SWE each particle i represents a column of water with a total mass m_i and carries its mass unchanged during the motion, so the total mass is exactly conserved. Moreover Bonet and Lok (1999) showed that the variational formulation here adopted conserves the momentum of the system in absence of external forces.

The kinetic energy for a system of particles can be approximated as the sum of energy of each particle:

$$K = \frac{1}{2}\sum_i m_i \left[\mathbf{v}_i \cdot \mathbf{v}_i + v_z^2 \right]; \qquad v_z = \mathbf{v}_i \cdot \nabla b_i \tag{6}$$

where $\mathbf{v}_i$ is the vector of the horizontal velocities and v_z is the vertical component of the velocity, the last term is usually neglected in the classical SWEs, but due to the Hamiltonian approach it is possible to include it in our analysis.

The potential energy of each column of water can be defined at the baricenter (this is because of the hydrostatic pressure distribution) and it can be expressed as a sum of the external and internal energy of each particle:

$$\pi = \pi_{ext} + \pi_{int} = \sum_i m_i g b_i + \frac{1}{2}\sum_i m_i g d_i \tag{7}$$

where g is the gravity acceleration and b_i is the bottom elevation of particle i, π_{ext} is the external potential energy and π_{int} is the internal potential energy.

Appling the chain rule to Equations (6) and (7) after some algebra, it is possible to obtain the following expression of acceleration $\mathbf{a}_i$:

$$\mathbf{a}_i = \frac{g + \mathbf{v}_i \cdot \mathbf{k}_i \mathbf{v}_i + \mathbf{t}_i \cdot \nabla b_i}{1 + \nabla b_i \cdot \nabla b_i} \nabla b_i - \mathbf{t}_i \tag{8}$$

where $\mathbf{k}_i = \nabla\left(\nabla b_i\right)$ is the curvature tensor of $b(\boldsymbol{x})$, and $\mathbf{t}_i$ is the acceleration due to the internal force. $\mathbf{t}_i$ is calculated using the continuity equation and the internal energy expressed in terms of energy per unit mass (Bonet and Lok 1999):

$$\boldsymbol{t}_i = \sum_j m_j \frac{g}{2\rho_w} \left(\frac{\nabla W_j(\mathbf{x}_i, h_j)}{\alpha_j} - \frac{\nabla W_i(\mathbf{x}_j, h_i)}{\alpha_i} \right) \tag{9}$$

where α is a correction factor due to the variable smoothing length:

$$\alpha_i = -\frac{1}{\rho_i d_m} \sum_j m_j r_{ij} \frac{dW_{ij}}{dr_{ij}} \tag{10}$$

where r_{ij} is the distance between particle i and j.

2.3 *Slope source term*

In order to deal with arbitrarily complex bathymetries we introduce a general method for discretizing the bed gradient source term based on an SPH interpolation technique. We thus discretize the two terms ∇b_i and $\boldsymbol{k}_i$ by an SPH interpolation.
This interpolation is performed using not the fluid particles but a new set of interpolation points called bottom particles. These points are introduced at the beginning of the simulation, they are distributed on a Cartesian uniform grid over the domain and they do not move during the simula-

tion. The only physical quantity associated with bottom particles is the bottom height b and an associated volume V_j (Vacondio et al. 2009b).
The bottom elevation of the i-th fluid particle b_i is calculated using an SPH summation formula using the bottom particles:

$$b_i = \sum_j b_j^b \bar{W}_i(\mathbf{x}_i - \mathbf{x}_j^b, h^b) V_j \tag{11}$$

where b_j^b indicates the bottom elevation of the j-th bottom particle located at $\mathbf{x}_j^b$, h^b is the constant smoothing length of bottom particles and $\bar{W}_i$ is the kernel for i-th particle corrected using a Shepard filter. The gradient of the bottom ∇b_i is evaluated using an SPH interpolation together with the gradient kernel correction proposed by Bonet & Lok (1999):

$$\nabla b_i = \sum_j b_j^b \tilde{\nabla} W_i(\mathbf{x}_i - \mathbf{x}_j^b, h^b) V_j \tag{12}$$

where $\tilde{\nabla} W_i$ is the corrected gradient of the kernel. Finally the curvature tensor $\boldsymbol{k}_i$ is derived using the following integral approximation (Monaghan 2005):

$$\left(\frac{\partial^2 b}{\partial x^\alpha \partial x^\beta}\right)_i = \sum_j \left(4\frac{x_{ij}^\alpha x_{ij}^\beta}{r_{ij}^2} - \delta^{\alpha\beta}\right)\frac{b_i - b_j^b}{\mathbf{r}_{ij}\cdot\mathbf{r}_{ij} + \eta^2}\mathbf{r}_{ij} \cdot\tilde{\nabla} W_i(\mathbf{x}_i - \mathbf{x}_j^b, h^b) V_j \tag{13}$$

where α and β are two generic coordinates and $\eta = 0.01h^b$, $\mathbf{r}_{ij} = \mathbf{x}_i - \mathbf{x}_j^b$.

2.4 *Particle splitting*

The main problem in the SPH-SWE scheme the lack of resolution when the fluid moves into very shallow water or over an initially dry bottom because the variable smoothing length is inversely proportional to water depth (Equation 3) and it causes poor resolution at small depths. To overcome this problem a refinement procedure has been developed: if a particle i has an area $A_i = m_i/\rho_i$ greater than a threshold value it is split into 7 daughter particles.

Feldman & Bonet (2007) defined a dynamic splitting procedure for particles in SPH models for Navier-Stokes equations which is conservative, and is suitable also for multidimensional domains but without considering the variable smoothing length. In this work we adapt their procedure to our SWE model with a new extension taking into account also the effects of the variable smoothing length; the details of this procedure are not reported here for lack of space but they are available in Vacondio et al. (2009a). The key idea is to define a refinement algorithm able to conserve both the mass and the momentum and to minimize the error in the density and velocities fields: once the number of daughter particles and their relative position are defined, then their masses are calculated solving a model problem that guarantee the minimization of the error in the density field.

3 TEST CASES

3.1 *Circular dam break on a non-flat bottom*

The SPH discretization of the bed gradient source term presented in section 2 is tested against the reference solution of a frictionless circular dam break with non-flat bottom (Aureli et al. 2008a). A cylindrical water volume of radius R_0 = 10 m is initially placed in a circular domain of radius R = 25 m centered in (x = 0, y = 0); the water is initially at rest. The bottom profile is described by the following equation:

$$z(r) = 0.5\left[1 + \cos\left(\frac{2\pi}{5}r\right)\right] \tag{14}$$

where $r = \sqrt{x^2 + y^2}$ is the radius.

The reference solution for this test case is calculated solving a 1D inhomogeneous problem along the radial direction by means of a Finite Volume code using a very fine mesh with a cell size of 0.005 m.

The SPH numerical solution has been obtained using 126,688 fluid particles and 1,040,400 bottom particles in describing the bed slope source term, this corresponds to an initial particle distance of 0.05 m. Figure 1 shows the numerical profiles of water level at x=0 and x=y at some selected times compared with the reference solution; even if some difference can be noticed at time 2s in the region close to the boundary, the SPH code is able to reproduce the reference solution in a satisfactory way. Moreover there is no difference between the two profiles at x=0 and x=y, this means that the numerical solution is able to keep the radial symmetry of the test case.

3.2 *CADAM test case with a 45° bend*

The European Concerted Action on DAm break Modelling (CADAM) conducted an experiment where a dam break flow occurs along an initially dry channel (Soares Frazão et al 1998). The channel has a rectangular cross section of 0.495 m, is connected upstream with a square reservoir and is 8.4 m long. A 45° bend is located at 4.25 m, the bottom is 0.33 m higher than the one of the reservoir, as plotted in Figure 2. The water levels are registered during the experiment in the reservoir and along the channel using 9 gauges. This case

has been used extensively by other SWE researchers (Liang and Borthwick 2009, Zhou et al. 2004) for benchmarking since it has a variety of difficult aspects.

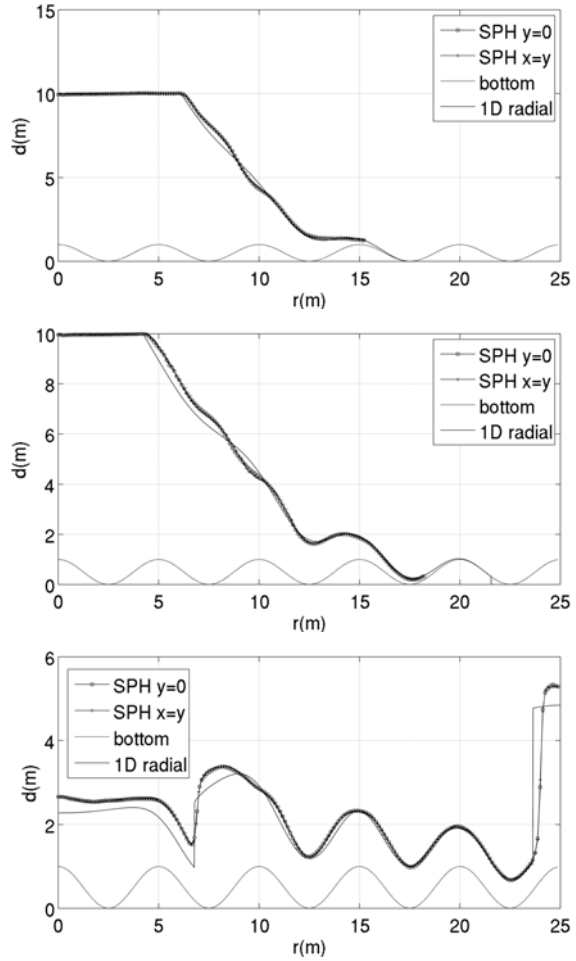

Figure 1. Circular dam break over a non-flat bottom: comparison of water depth between SPH results at x=0 and x=y and 1D radial reference solution at times: 0.4 0.6 and 2s

A first simulation is performed using no refinement and 9,603 particles are initially positioned in the reservoir, the Manning coefficient of the friction source term is taken as $n = 0.01\text{s m}^{-1/3}$. In order to reduce the computational time a second simulation is performed using bigger particles inside the reservoir and splitting them when they approach the channel: 2,450 particles are initially placed in the reservoir.

The step located between the bottom of the reservoir and the channel has been discretized using the SPH interpolation method of bottom particles (Vacondio et al. 2009b), the only expedient introduced here is a smoothing length for the bottom particles which is two times the smoothing length initially assigned to the fluid particles. Figure 3 shows the comparison between the experimental and numerical water levels obtained with and without the splitting procedure: gauge 1 is placed inside the reservoir near the channel inlet; the good agreement of registered data with the numerical results means that the discharge that is entering in the channel is correct. Gauges 2 and 4 are placed along the channel upstream the bend, therefore they registered the abrupt water level elevation due to the reflected wave that is travelling upstream to the reservoir. The numerical model is able to reproduce the water level at gauges 4 and at gauge 2 after 20 s whereas there is a difference with the experimental data of gauge 2 in the first half of the experiment. This difference is presents also in the results obtained using Eulerian numerical schemes (Soares Frazão et al 1998) and therefore can not be ascribed to the SPH-SWEs scheme presented in this paper.

Gauges 5 and 7 are placed in the bend and the numerical model is able to reproduce these registered water levels, in particular the surface inclination in the bend is correctly simulated. Gauge 9 is placed downstream of the bend and the overall comparison of the water level is satisfactory although the numerical model slightly underpredicts the water level.

Despite of the reduced resolution the results of the simulation with splitting procedure activated are analogous to the results obtained without it, where more particles are used. This is due to the splitting procedure adopted that increases the resolution just in the part of the domain where the strong changes in the water depth and in the velocity field occur. The computational time of the simulation with no refinement is 147 minutes, whereas it is equal to 86 minutes in the simulation with bigger particles and refinement procedure: therefore with the refinement procedure the computational time is reduced of 40%.

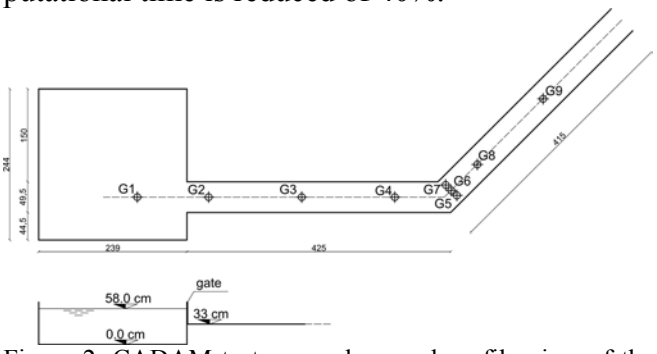

Figure 2. CADAM test case: plane and profile view of the experimental setup

3.3 *2D dam break tests with image technique acquisition*

Aureli et al (2008b) made a set of experimental test cases where a 2D dam break is reproduced in the experimental facility showed in Figure 4.

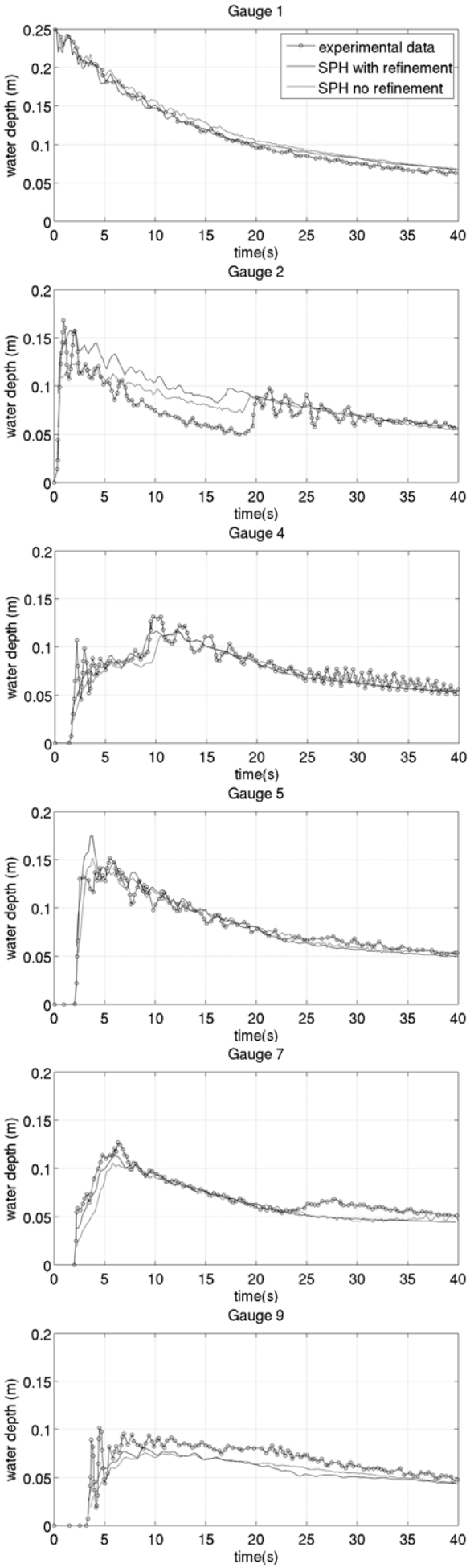

Figure 3. CADAM test case: experimental and numerical water depth time series at different gauges.

A rectangular tank is divided into two parts: the smaller functioning as a reservoir and the larger designed to receive the flood wave after the sudden removal of a gate placed in the middle of the dividing wall.

The data are collected by means of an imaging technique procedure and the maps of the registered water depth in the larger right-hand part of the tank are available at different time steps; in this section a comparison between the experimental and the numerical maps is shown in order to validate the SPH-SWEs numerical code.

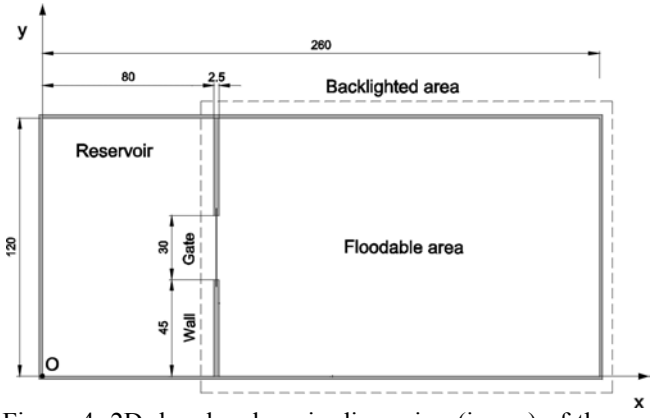

Figure 4. 2D dam break main dimension (in cm) of the experimental facility.

Two different tests are presented: in the first one, the water at rest is placed just in the small reservoir and the initial water depth is 6.3 cm whereas the floodable area is initially dry. In the second test case the initial water depth is 15 cm in the small reservoir and 1 cm in the big one. The presence of an initially wet bottom causes the formation of a shock that moved downstream and, after a few seconds, was reflected by the walls of the experimental facility.

The numerical simulation of the first test was done using 38,560 particle initially placed in the small reservoir; the Manning coefficient is taken as $n = 0.007$ s m$^{-1/3}$ and a splitting procedure has been applied just before the particles enter in the floodable area: this assures an higher resolution in the floodable area without increasing the number of particles in the reservoir. Figures 5 – 8 show the comparison between numerical and experimental maps of water elevation in the floodable area at times 0.38, 1.22, 2.21 and 2.88 s. The numerical model is able to correctly reproduce the flow expansion, also the shock wave generated by the impact against the lateral and the downstream walls are correctly reproduced by the numerical model. Figure 9 shows the water depth map at time 0.38 s without refinement; comparing it with Figure 5, it can be observed that the results obtained using the splitting procedure are more similar to the experimental map therefore the particle splitting procedure is effective in increasing the accuracy of the results.

In the second test the wet dam break has been reproduced and 44,419 particles have been used in the simulation. No splitting procedure has been adopted because the floodable area is already filled with particles at the begin of the simulation and this automatically reduce the lack of resolution during the flooding.

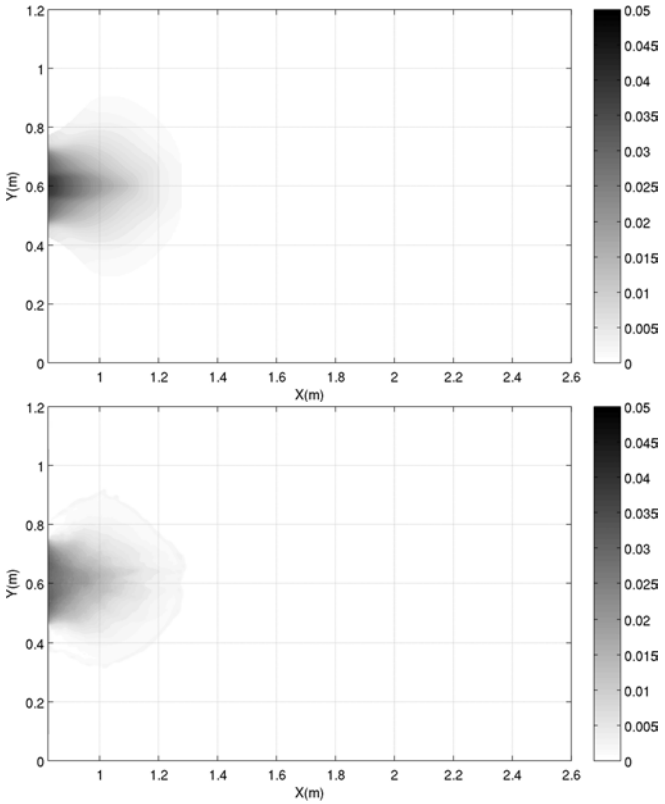

Figure 5. 2D dam break 1: numerical (above) and experimental (under) water depth maps at time 0.38 s.

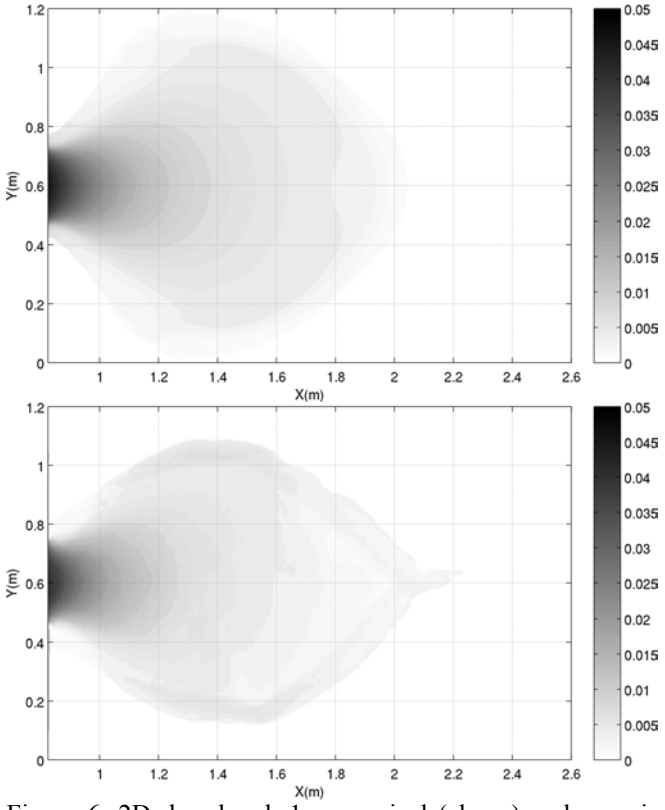

Figure 6. 2D dam break 1: numerical (above) and experimental (under) water depth maps at time 1.22 s.

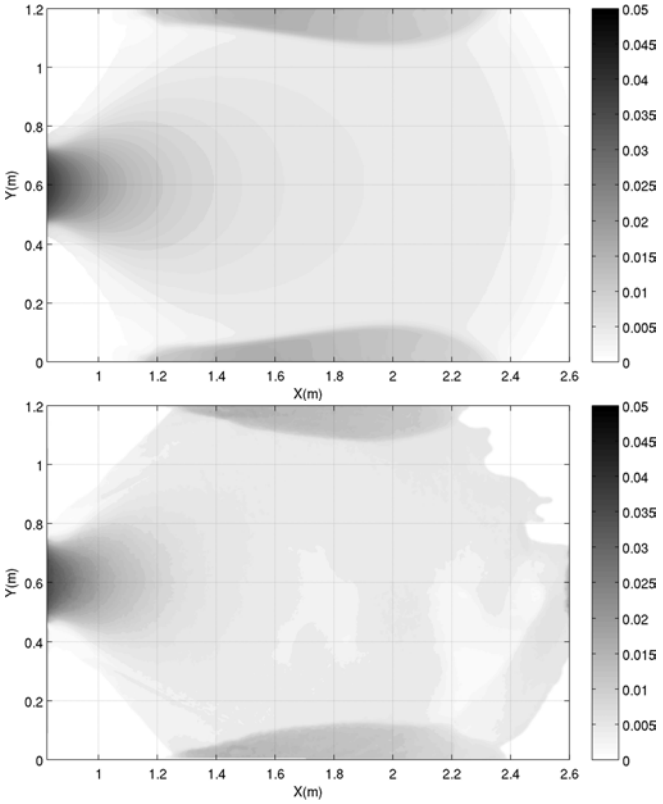

Figure 7. 2D dam break 1: numerical (above) and experimental (under) water depth maps at time 2.21 s.

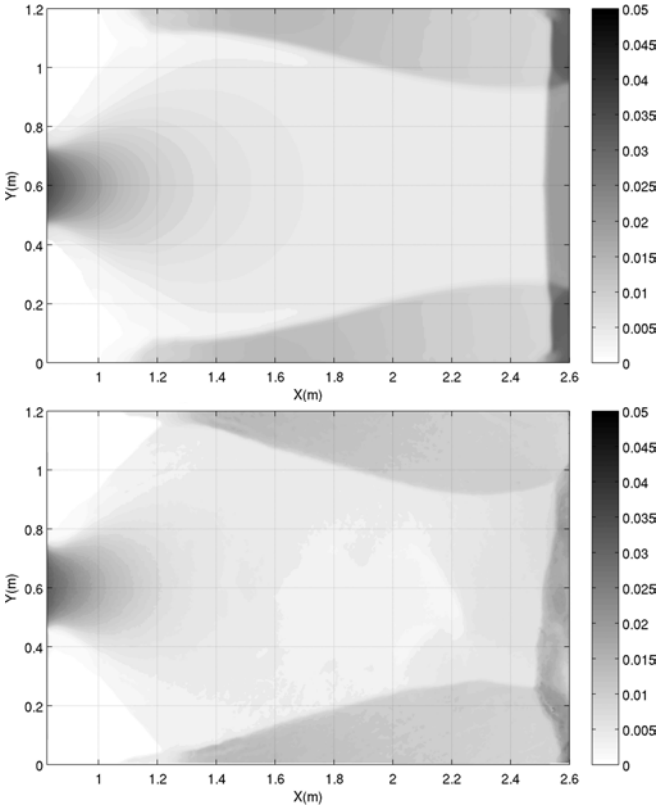

Figure 8. 2D dam break 1: numerical (above) and experimental (under) water depth maps at time 2.88 s.

Figures 10 – 13 show the comparison between numerical and experimental maps of water elevation in the floodable area at times 0.59, 1.29 and 2.00 and 2.70 s. Some discrepancies are due to the presence of breaking waves in the experimental data in Figure 10 and 13, clearly these cannot be directly reproduced by SWE model. Moreover the

position of the shock wave travelling upstream in Figure 12 is slightly different in the numerical and the experimental maps. Despite these minor discrepancies, the numerical model is able to reproduce the main features of the phenomena: the water elevation at different time steps and the position of the shock waves before and after the impact against the walls.

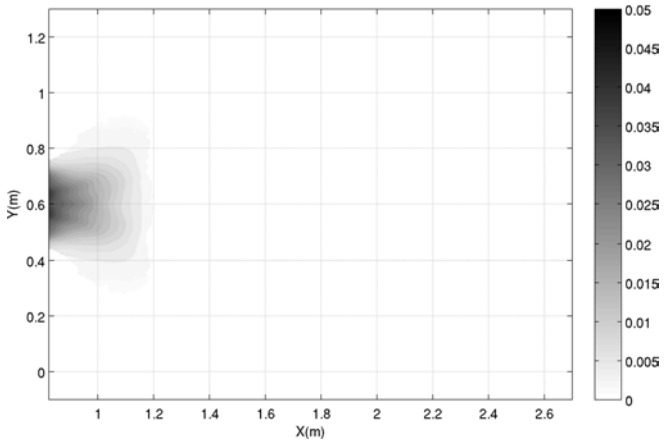

Figure 9. 2D dam break 1: numerical water depth maps without refinement at time 0.38 s.

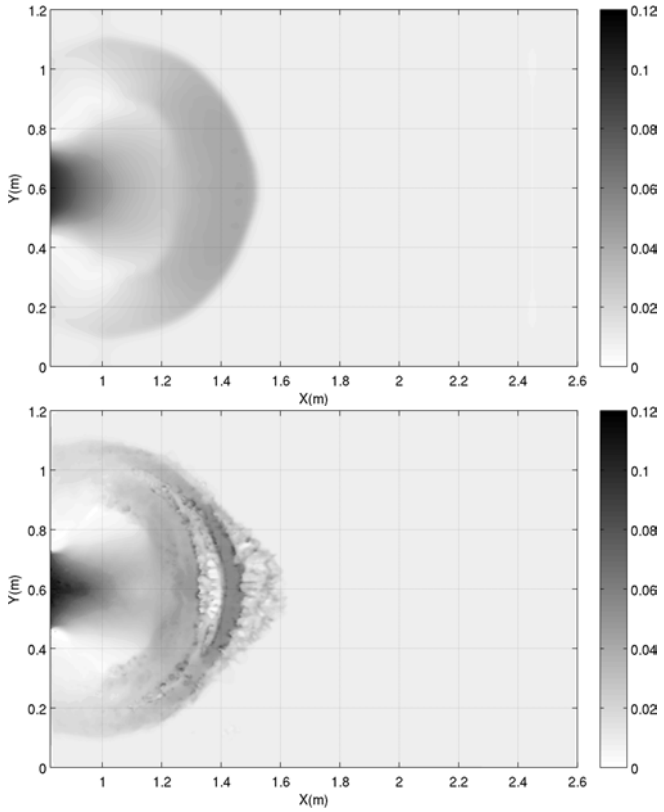

Figure 10. 2D dam break 2: numerical (above) and experimental (under) water depth maps at time 0.59 s.

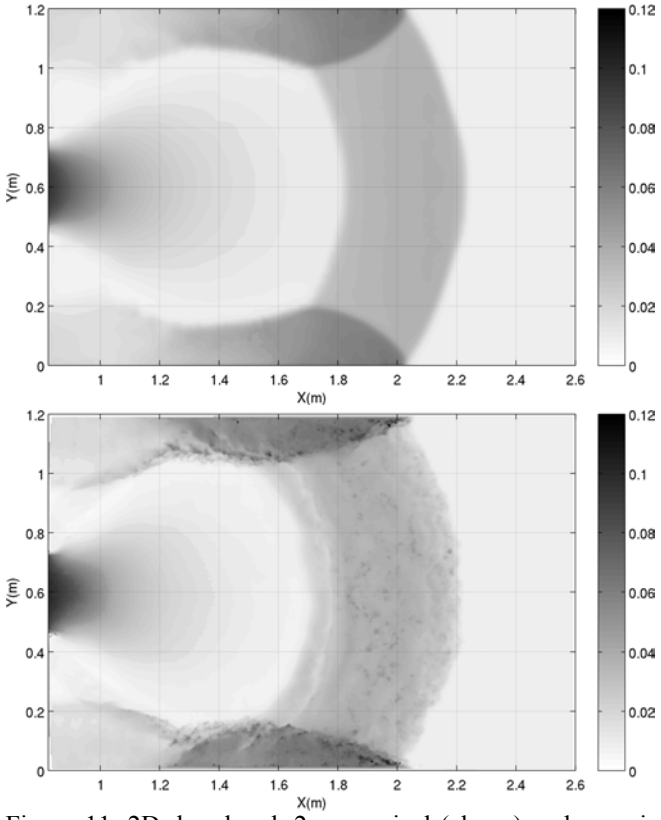

Figure 11. 2D dam break 2: numerical (above) and experimental (under) water depth maps at time 1.29 s.

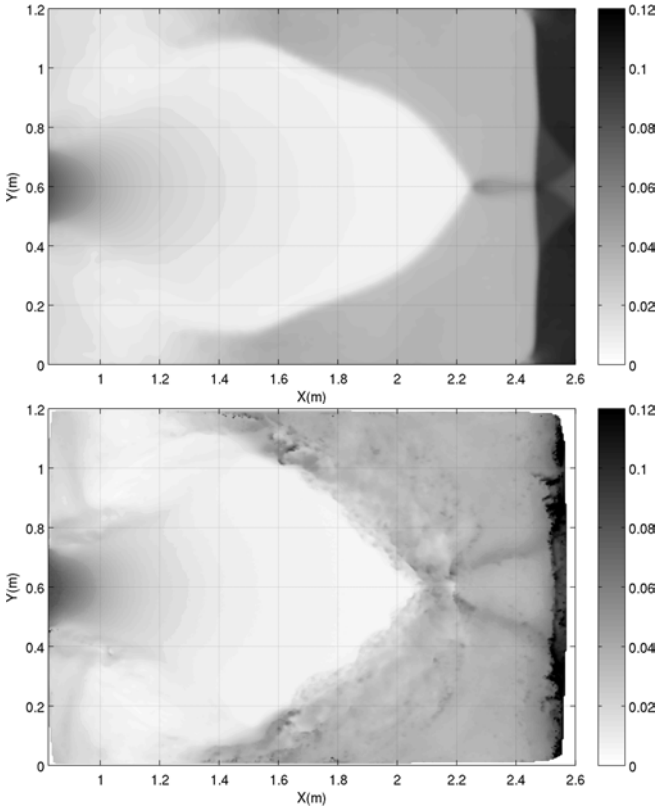

Figure 12. 2D dam break 2: numerical (above) and experimental (under) water depth maps at time 2.00 s.

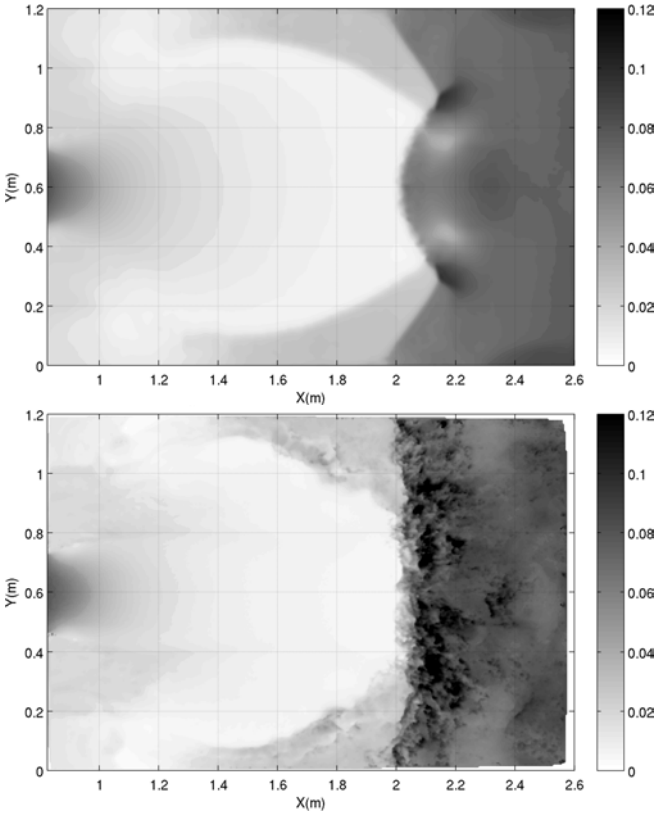

Figure 13. 2D dam break 2: numerical (above) and experimental (under) water depth maps at time 2.70 s.

4 CONCLUSION

In this paper an SPH method for numerical discretization of shallow water equations has been presented. Previously the main limitation of this numerical scheme was the lack of resolution in zones with a reduced water depth; this has been overcome in this paper by introducing a particle splitting procedure: if one particle has an area which is more than a fixed value it is divided into seven daughter particles. The masses, velocities and water depth of daughter particles are assigned by conserving both the mass and momentum. In order to extend the method to real case problems another improvement has been made: the slope source term is calculated by means of a SPH interpolation method which can be applied for any bathymetry.

In order to show the capability of the SPH-SWEs numerical model to reproduce rapidly varying flow, It has been tested against a reference solution and two experimental test cases and its capability obtaining good agreement with the reference solutions.

In future works the open boundaries will be introduced in the code and real flooding events will be reproduced.

REFERENCES

Aureli, F. Maranzoni, A. Mignosa, P. Ziveri, C. 2008. A weighted surface-depth gradient method for the numerical integration of the 2d shallow water equations with topography- Advances in Water Resources, 31 (7), 962-974.

Aureli, F. Maranzoni, A. Mignosa, P. Ziveri, C. 2008. Dam-Break Flows: Acquisition of Experimental Data through an Imaging Technique and 2D Numerical Modeling. Journal of Hydraulic Engineering, 134 (8), 1089-1101.

Benz, W. 1990. Smooth particle hydrodynamics - a review. In: R. J. Buchler (Ed.), Proceedings of the NATO Advanced Research Workshop on The Numerical Modelling of Nonlinear Stellar Pulsations Problems and Prospects, Kluwer Academic Publishers.

Bonet, J. L. Lok, T. S. 1999. Variational and momentum preservation aspects of smooth particle hydrodynamic formulations. Computer Methods in applied mechanics and engineering 180, 97-115.

De Leffe, M. Le Touzé, D. Alessandrini, B. 2008. Coastal flow simulations using an sph formulation modelling the non-linear shallow water equations. In: Proc. 3th ER-COFTAC SPHERIC workshop on SPH applications, Lausanne, Switzerland, 48-54.

Feldman, J. Bonet, J. , 2007. Dynamic refinement and boundary contact forces in SPH with applications in fluid flow problems. International Journal for Numerical Methods in Engineering, 7 (3), 295-324.

Liang, Q. Borthwick, A. G. L. 2009. Adaptive quadtree simulation of shallow flows with wet-dry fronts over complex topography. Computers & Fluids, 38 (2), 221-234.

Monaghan, J. J., 1992. Smoothed particle hydrodynamics. Annual review of Astronomy and Astrophysics, 30, 543-574.

Rodriguez-Paz, M. Bonet, J. 2005. A corrected smooth particle hydrodynamics formulation of the shallow-water equations. Computers & Structures, 17-18, 1396-1410.

Soares Frazão S., Sillen X., Zech Y., 1998. Dam-break flow through sharp bends physical model and 2d boltzmann model validation. In: Proc. of the 6. Summary and conclusions CADAM meeting, Wallingford, United Kingdom, 2 and 3 March 1998, Commission Europenne, Bruxelles, 151-169.

Vacondio, R. Rogers, B. D. Stansby, P. K. 2009. An SPH shock capturing method for shallow water flows with particle splitting. Journal of Computational Physics - Submitted.

Vacondio, R. Rogers, B. D. Stansby, P. K. 2009. Smoothed particle hydrodynamics: approximate zero-consistent 2-d boundary conditions and still shallow water tests. Computers & Fluids - Submitted.

Zhou, J. G. Causon, D. M. Mingham, C. G. Ingram, D. M. 2004. Numerical prediction of dam-break flows in general geometries with complex bed topography. Journal of Hydraulic Engineering, 130 (4), 332-340.